

promoting access to White Rose research papers



Universities of Leeds, Sheffield and York
<http://eprints.whiterose.ac.uk/>

This is the Author's Accepted version of an article published in **Proceedings of the Royal Society A: Mathematical, Physical and Engineering Sciences Physical and Engineering Sciences**

White Rose Research Online URL for this paper:

<http://eprints.whiterose.ac.uk/id/eprint/78119>

Published article:

Hughes, KJ, Brindley, J and McIntosh, AC (2013) *Initiation and propagation of combustion waves with competitive reactions and water evaporation.*

Proceedings of the Royal Society A: Mathematical, Physical and Engineering Sciences Physical and Engineering Sciences, 469 (2160). 20130506. ISSN 1364-5021

<http://dx.doi.org/10.1098/rspa.2013.0506>

Initiation and Propagation of Combustion Waves with Competitive Reactions and Water Evaporation

K.J. Hughes¹, J. Brindley² and A.C. McIntosh¹

¹Energy Technology and Innovation Initiative, University of Leeds, Leeds, LS2 9JT, UK

²School of Mathematics, University of Leeds, Leeds, LS2 9JT, UK

Abstract

We use a one dimensional model to present numerical and analytical results on the propagation of combustion waves, driven by competing exothermic and endothermic chemical reactions in parallel with water evaporation. The research was motivated by the phenomenology of emulsion explosives comprising a mixture of fuel and an ammonium nitrate(AN)-water solution. An extensive programme of computational modelling has covered a range of important physical influences, particularly the water fraction and the ambient pressure, on which the endothermic effect of evaporation is critically dependent. A substantial, and not immediately obvious, influence of the evaporation, through its effect on the temperature, is on the fraction of the AN consumed respectively by the competing exo and endothermic reactions, which are controlled by differing, temperature-sensitive kinetics. Self-sustaining travelling combustion waves are initiated for a wide range of parameter values. They are usually oscillatory, regular for small water content and becoming highly irregular, sometimes causing extinction for larger water content. The numerics are complemented by a brief theoretical analysis, which throws light on the complex and subtle interplay of the two chemical reactions and the evaporation, expressed in the form of a highly convoluted integral over the whole time and space extent of the process.

1 Background and Motivation.

The research described here was motivated by the ignition and subsequent burning behaviour of ammonium nitrate (AN) based emulsion mixtures, of which experimental and observational results reveal aspects of behaviour which are not fully understood [1-3]. The emulsions usually consist of a water/AN solution and a hydrocarbon fuel, with, in most cases, other additives. The salient qualitative features are those of a minimum burning pressure (MBP), below which steady, self-sustained burning is impossible, together with, where steady burning is possible, the creation of a self-propagating combustion wave driven by the overall net exothermic processes of decomposition and dissociation of the AN. This is then a precursor of a subsequent much more energetic, possibly explosive, oxidation of the fuel.

Ammonium nitrate (AN) is a basic component of many materials deliberately manufactured as explosives, and also of many other industrial chemicals, especially agricultural fertilisers, where the possibility of fire or explosion during the production, storage and transport processes is a major safety consideration. For example, in the explosives industry, the phenomenology of

ignition and combustion of AN based emulsion explosives used in mining operations is of great importance; in the agricultural chemical industry the potential fire and/or explosion dangers associated with accidental “hotspots”, caused by mechanical or electrical malfunction, or of “spontaneous” ignition and combustion of bulk volumes of materials in transport or storage, are of major concern.

The decomposition/dissociation processes constituting the initial “burning” of AN, either by itself or in various compounds and mixtures, have been widely studied experimentally and modelled, both numerically, and to a lesser extent, analytically [4-7]. Despite its importance, the kinetics of AN decomposition have defied consistent experimental evaluation in terms of a single one-step Arrhenius representation. More recently, modellers have taken into account not only the dominant exothermic decomposition process, but also a concurrent endothermic dissociation process feeding *competitively* on the initial AN [8,9]. Though some measure of agreement between observations and numerical/theoretical results has been achieved, there is as yet no full understanding of the interplay of the complex exothermic and endothermic processes involved, nor of their response to external forcing. These uncertainties make exact *simulation* of the phenomenology impracticable, and our approach here is that of *modelling*, in which we identify *qualitative* characteristics and trends in a way that enables them to be associated confidently with physical properties and external forcing

Our aims in this paper are therefore to construct a mathematical/numerical model for AN decomposition which represents the dominant physical and chemical features of the actual process, to explore the phenomenology predicted by the model, and to relate it to the observed behaviour of real systems, identifying the important underlying physical and chemical properties and influences. These aims may be approached through an iterative process of model refinement, and suggest a hierarchy of models incorporating, progressively, the various features of the experimental configurations and observations, e.g. geometry, heat losses, mixture characteristics (water/AN ratio, particulate additives, heterogeneity), chemical kinetics, in a way that permits the effect of each to be separately identified.

In Section 2 of this paper we introduce and describe in some detail the model we have used together with our strategy and methodology. Section 3 comprises the main numerical results, whilst in Section 4 we present a brief complementary theoretical investigation. Finally, in Section 4 we summarise and discuss the main results.

2. Modelling Approach and Methodology

As is the case in most physico-chemical phenomena, the observed behaviour is the consequence of many concurrent or consecutive individual reactive processes, some of which are exothermic and some endothermic. A full representation of even the simplest chemical system comprises a great number, typically hundreds, of individual reactions, and is amenable only to massive computational modelling. Much useful understanding and even prediction of qualitative behaviour may however be gained by considering much simpler “lumped” models which reproduce the essential phenomenology.

In our case, in which the thermal consequences of the reaction are important, the simplest useful model comprises just two concurrent reactions, one exothermic and one endothermic, having different chemical kinetics. These feed on the same initial reactant material, and so are *competitive reactions*, in contrast to *parallel reactions*, in which each reaction consumes a distinct and separate component of the initial reactant [10]

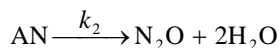
The phenomenology of parallel reactions has received a good deal of modelling attention, particularly in the context of flame propagation or extinction by an endothermic reaction, see for example Gray *et al.* [11], Simon *et al.* [12], and references therein; the case of competitive

reactions, typical of decomposition or dissociation processes, has received much less attention. In recent papers [13-15] we have explored the behaviour exhibited by a model system in which a competitive endothermic reaction is regarded as a perturbation to a coexisting exothermic reaction having a lower activation energy. There we were concerned with the existence and stability of travelling reaction fronts in a spatially one-dimensional distribution of reactant material. The work reported here seeks to explore more fully the phenomenology of ignition and front initiation, structure and propagation in AN, regarded as a competitively reacting material, when a parallel endothermic process, is also present. In this work, we have added a specific heat loss due to water evaporation, and the results have some similarity to earlier research for combustion waves with heat loss [16, 17].

The extensive literature on the decomposition of AN reveals a surprising variety of representations of the chemistry involved [4-7, 18], with differences between the condensed and molten phases, and showing evidence of autocatalysis in the molten phase; common to virtually all is the phenomenon of *competitive* processes feeding on the same initial AN resource. Importantly, some are exothermic and some endothermic. In reality, beyond a temperature threshold the overall decomposition process is exothermic. Here, in the interests of simplicity, we follow Brill *et al.* [4] in assuming just two concurrent competing processes, one endothermic



and one exothermic



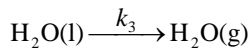
For simplicity these chemical processes are assumed to be pressure independent, with enthalpies of reaction that are temperature independent, and the rate coefficients k_1 and k_2 described by standard Arrhenius expressions. The parameter values are summarised in table 1, the activation energies are subsequently denoted by E_1 and E_2 respectively, the reaction enthalpies as Q_1 and Q_2 , and because of the notation used in the theoretical considerations described in section 4, the A-factors are referred to as K_1 and K_2 .

Table 1. AN decomposition Arrhenius parameters and enthalpies of reaction

reaction	A-factor (s^{-1})	Activation Energy (K)	Reaction Enthalpy ($\text{kJ}\cdot\text{mol}^{-1}$)
1	1.256×10^{15}	23754	184
2	5.985×10^8	12078	-38

The Arrhenius parameters for reaction one are derived from Sinditski *et al.* [5], and those for reaction two from Manelis *et al.* [18], with the A-factors multiplied by factors of 5 and 30 respectively, as discussed by Sinditski *et al.* [5] to represent the large effect of small quantities of additives. Q_1 is taken from Brill *et al.* [4], from which Q_2 is then derived by a Hess's law calculation (the enthalpy change accompanying a chemical change is independent of the route by which the chemical change occurs).

The rate at which water evaporation will occur in a real situation will depend on the detailed physics, especially the presence of nuclei for bubble formation. Here we assume that it may be represented by an appropriate smoothing function centred on P_{sat} . We have further assumed that everything takes place at constant ambient pressure, P_{amb} , consistent with the experiments referred to earlier, and that the gaseous products of the evaporation and dissociation take no further part in the process. Hence water evaporation is superficially handled in a similar fashion to the AN decomposition, in which it is treated as a normal chemical reaction with a first order rate coefficient,



However, k_3 is now a smoothed function of the saturation vapour pressure given by:

$$k_3 = \gamma(1 - 1/(1 + \exp((P_{\text{sat}} - P_{\text{amb}})/\alpha)))$$

where γ is a first order rate coefficient arbitrarily set at 1 s^{-1} , P_{amb} is the constant ambient pressure, and P_{sat} is the saturated vapour pressure which is a function of temperature. The smoothing function is sigmoidal, effectively switching off k_3 when P_{sat} is less than P_{amb} . The parameter α controls how sharply the sigmoidal function varies with P_{sat} , its units are the same as pressure, its value is arbitrary and we have used a value of 50 torr. The variation of P_{sat} with temperature is given by the numerical representation of Wagner [19] as

$$\ln(P_{\text{sat}}/P_c) = (T_c/T) \times (a\tau + b\tau^{1.5} + c\tau^3 + d\tau^6)$$

where

$$\tau = 1 - T/T_c$$

T_c and P_c are the critical temperature and pressure of water, and the variables a , b , c and d in the case of water are -7.77224, 1.45684, -2.71942 and -1.41336 respectively [19]. The latent heat of evaporation of water, Q_3 , is also temperature dependent, and is given by the numerical representation of Pitzer [20] as

$$Q_3/RT_c = 7.08 \times (1 - T/T_c)^{0.354} + 10.95 \times w \times (1 - T/T_c)^{0.456}$$

where for water, w is 0.344. In practice, these saturation vapour pressure and latent heat parameters for a mixture will be somewhat different to pure water, but we should not expect any qualitatively different behaviour.

The physical process of evaporation of the liquid is therefore very strongly temperature and pressure dependent, and it is this, endothermic, process, and its interaction with the competing dissociation processes for AN, which is crucial to the behaviour of the system when heated. These competing processes are illustrated schematically in Figure 1.

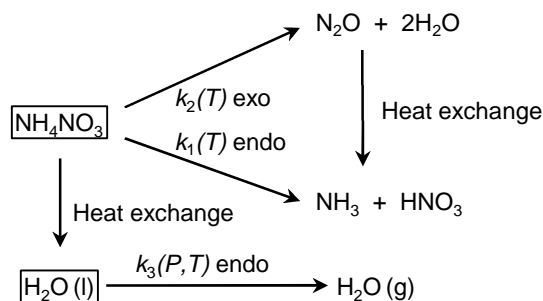


Figure 1. Schematic representation of the competing system processes

Depending on the strength and form of the initial heat source, the fraction of water and the ambient pressure, it may or may not be possible for a localised heat source to initiate a self-propagating burning front in which case the whole of the AN is consumed, leaving, when other heat losses are ignored, a “plateau” burnt temperature, T_b , behind the moving front.

Model Equations

Based on the assumptions above, the equations for AN and water, together with an energy equation for the whole mixture, may be written as follows

$$\frac{\partial[AN]}{\partial t} = -(k_1 + k_2)[AN] + D_{AN}\nabla^2[AN] \quad (1)$$

$$\frac{\partial[Water]}{\partial t} = -k_3[Water] + D_{Water}\nabla^2[Water] \quad (2)$$

$$\frac{\partial T}{\partial t} = \frac{-(Q_1k_1[AN] + Q_2k_2[AN] + Q_3k_3[Water])}{C_v\rho} + D_T\nabla^2T \quad (3)$$

In the current implementation of this model, we have assumed no diffusion of AN or water, therefore the diffusion coefficients D_{AN} and D_{Water} are set to zero. The specific heat of the emulsion C_v and emulsion density ρ are assumed to be constant, and D_T , the temperature diffusivity, is given by: $D_T = \lambda/\rho C_v$. The value of λ , the thermal conductivity, is taken as $0.004 \text{ W}\cdot\text{cm}^{-1}\cdot\text{K}^{-1}$, ρ is taken to be $1.4 \text{ g}\cdot\text{cm}^{-3}$ and the heat capacity as $1.7 \text{ J}\cdot\text{g}^{-1}\cdot\text{K}^{-1}$ [2,3].

We have explored sensitivities of results to variations in some of the parameters. Note that values quoted in the literature for the chemical kinetics, especially for mixtures containing active additives, are subject to considerable uncertainty and vary widely. To a much smaller extent this is also true of the values for latent heat of evaporation for AN/water mixtures [21], but for simplicity we have used the well-known results for temperature dependence of latent heat for evaporation of pure water [20]. The effects of small amounts of additives have been modelled by adjustments to the reaction rate coefficients as described previously.

Initial and Boundary Conditions

The initial compositions for the emulsion have ranged from zero water up to 30 % water (on a molar basis), the rest being (dissolved) AN. In all cases an initial temperature of 300 K has been assumed. In the 1-dimensional spatially varying model the left hand, cold, boundary, at $x = 0$, is held at constant temperature 300 K throughout. The right hand boundary at $x = 100$ is heated by a constant energy input of $20 \text{ W}\cdot\text{cm}^{-2}$ applied for 35 s, after which a zero temperature gradient is imposed (no heat transfer).

Numerics

A Fortran code based on the NAG library routine D03PSF has been used [22, 23]. This routine integrates a system of linear or nonlinear convection-diffusion equations in one spatial dimension, with optional source terms and scope for coupled ODEs. Typically, 1000 mesh points were employed, with an adaptive spatial mesh implemented in order to follow the progression of the propagating reaction front, based on a 2nd derivative function of the temperature using the default methodology implemented within the code. The frequency of remeshing is an adjustable parameter, and a balance between computational time requirements and code stability determines the optimal value of this parameter, from a series of tests this was set at 400 in these simulations.

3. Numerical Results

The simplest physical model we have considered is a “well-mixed”, or zero-dimensional, system, in which transport effects by diffusion or advection are neglected, gaseous and liquid phases are each uniformly spatially distributed and heat exchange between phases is assumed instantaneous, i.e. a single temperature field is assumed. Such a model can be useful only in modelling the initial ignition phenomenon and its dependence on mixture properties, chemical kinetics and ambient pressure. It does, however, give a feel for the influence of these features, and of the sensitive dependence of the phenomenology on the delicate interplay of a number of competitive processes. Conservation equations for AN in its basic dissolved state, water in liquid and vapour form, and fuel, together with an energy equation, then comprise a highly nonlinear set of ODEs containing numerous (and often uncertain) parametric representations of the physical and chemical processes involved. More detailed results will be published elsewhere, but the influence of pressure on the time to ignition is demonstrated in Figure 2, based on our computations, which shows clearly the existence of a practical cut off (for the kinetics assumed) at around 3 atmospheres, in accord with the phenomenon of an MBP, which has been observed in experiments and industrial practice [1-3].

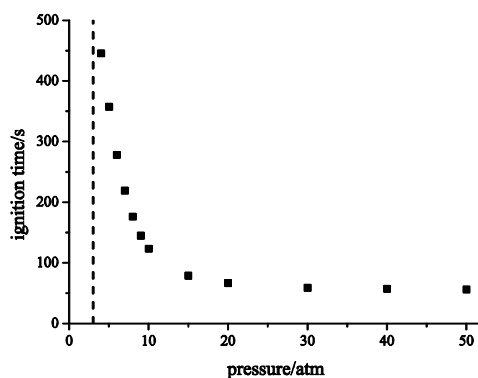


Figure 2. Numerically predicted ignition time as a function of ambient pressure in a zero dimensional model of AN ignition. Dashed line illustrates approximate cut-off for the ignition process.

The zero-dimensional results shown in Figure 2 clearly illustrate the important effects of ambient pressure on the dissociation of AN, and hence any subsequent fuel combustion. In the absence of external heat loss, the assumption of first order Arrhenius kinetics of course guarantees ultimate consumption of the AN provided that the water content is not too large; the actual time scale depends not only on the water content, with its ability to provide an endothermic “brake”, but also on the ambient pressure, which determines the temperature at which the brake is applied significantly.

In the more realistic spatial model on which this paper is based we have taken into account diffusion of heat, but at the same time concentrated on the phenomenology of the AN decomposition process, modelled as two *competitive* reactions, one exothermic and one endothermic, in the simultaneous presence of the *parallel* endothermic evaporation of the water content of the emulsion. This model is able to represent the creation, propagation and stability of travelling reaction fronts, and enables us to relate our results to the considerable literature on such fronts [16,24]. For simplicity we have assumed a spatially one-dimensional model, implicitly planar but readily extendable to cylindrical or spherical geometries. The extra refinements of, for example, mass diffusion, temperature differences between and heterogeneous distribution of the different components, external heat losses and more complex geometries, though doubtless important in the quantitative representation of the phenomenology

in particular cases, are neglected in the interests of clear exposure of the basic physico-chemical processes.

The numerical results display great sensitivity to parameter values, many of which, especially those relating to the chemical kinetics, are not known accurately, and which clearly depend on initial and boundary conditions. The dependency on initial conditions is only insofar as to establish a self-sustained combustion wave. However it is possible to recognise robust qualitative phenomenology and trends in behaviour which accord with experimental observations. In order to identify the effects of the several physical and chemical processes involved in the initiation and subsequent propagation of a dissociation front we have experimented with a hierarchy of models. The simplest retains only the exothermic component of the AN decomposition, ie $k_1 = 0$ in equation 1. In the absence of any heat losses, this model yields a travelling front, leaving in its trail a "plateau" burnt temperature, T_b . This gives a benchmark for a range of more realistic models involving AN reactions and water evaporation.

When values of the chemical kinetic parameters in k_1 and k_2 appropriate for "pure" AN were used it proved impossible to generate self-propagating fronts, even though initial ignition was sometimes possible; this accords with the extensive literature on AN combustion. However, for values modified to take a crude account of the effect of additives [5], travelling combustion fronts were observed to develop for wide ranges of initial conditions and ambient pressures. The usual structure consists of a precursor front at which the AN decomposes with a net exothermic effect, and, depending on ambient pressure, some or all of the water content evaporates, establishing a plateau temperature from which a fuel-oxidant reaction would subsequently raise the temperature further in a following front. The criterion for self-propagation of these fronts after the external forcing has been switched off is an important objective, clearly dependent on water fraction and ambient pressure, but also on the often poorly known values of several parameters, especially reaction rate coefficients, which can be massively influenced by quite small amounts of additives. Nevertheless we have found both self-propagation and extinction for parameter values well within the ranges quoted in the literature (for example Figures 3,4). A common feature of the dissociation fronts is the oscillatory nature of their propagation as illustrated in Figure 3, which shows the evolution in time of the temperature profile of the travelling AN combustion front for different water content.

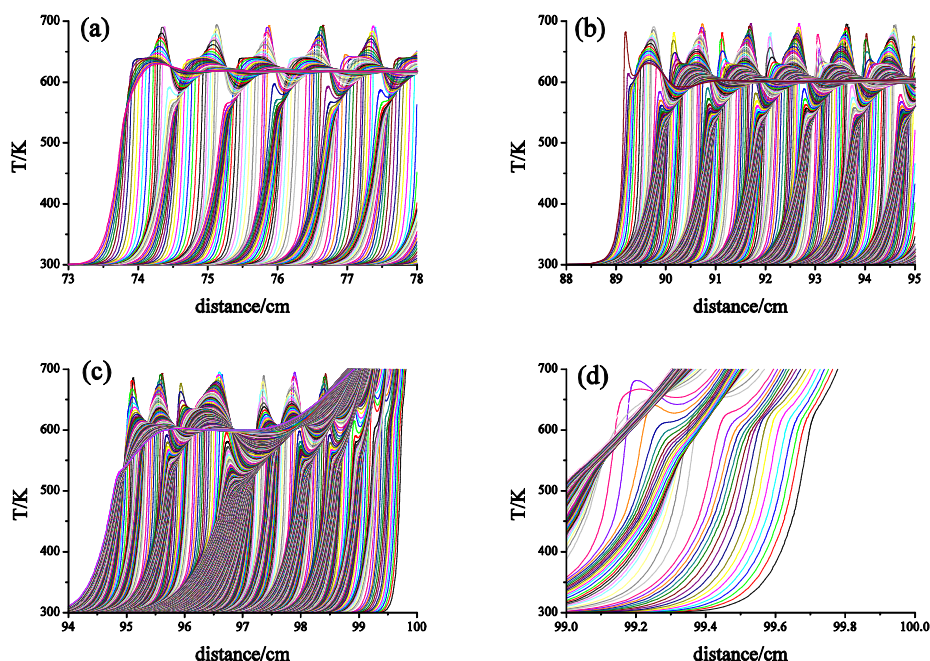


Figure 3. Temperature profiles at successive time intervals of the travelling AN combustion front at ambient pressure of 10 atm (a) – 5 % water, (b) – 10 % water, (c) – 15 % water, (d) – 20 % water

As the water fraction increases from 5 %, the behaviour becomes more irregular but apparently self-propagating, until at 20 % the initial ignition fails to propagate beyond a very small distance from the heat source. This accords with the predictions of earlier modellers of travelling combustion waves with heat loss [16] for the parameter ranges involved, and has been reproduced in an analytical model for the present system [14]. It is questionable whether or not such oscillations would be noticed experimentally; the plateau temperature left behind at c600 K is the obvious feature.

In the case of 1 % water however the front propagates through many oscillations before finally dying, as illustrated in Figure 4.

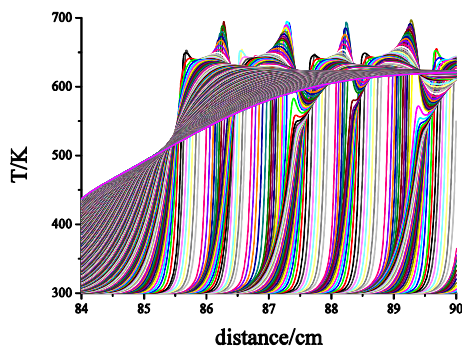


Figure 4. Temperature profile of the travelling AN combustion front at ambient pressure of 10 atm and 1 % water content.

This apparently anomalous behaviour, that more water can aid propagation, seems to occur for small water content over a range of ambient pressures. It also appears to be possible in the theoretical model discussed in Section 4. The physical mechanism for the behaviour is the delicate interplay of the two competing decomposition processes and the water evaporation, with its ability to affect the share of the decomposing AN between the competing exothermic and endothermic channels. A complete description of all our experimental results is not possible here, but diagnosis of a typical case illustrates the important competing processes.

With this in mind we examine a case in which a multiple-structured combustion front is seen to propagate. Figure 5 and Figure 6 show the spatial structure and evolution in time of the values of temperature and AN and water concentrations at two states in the cycle of oscillation, near the spatial positions of maximum and minimum frontal temperature respectively.

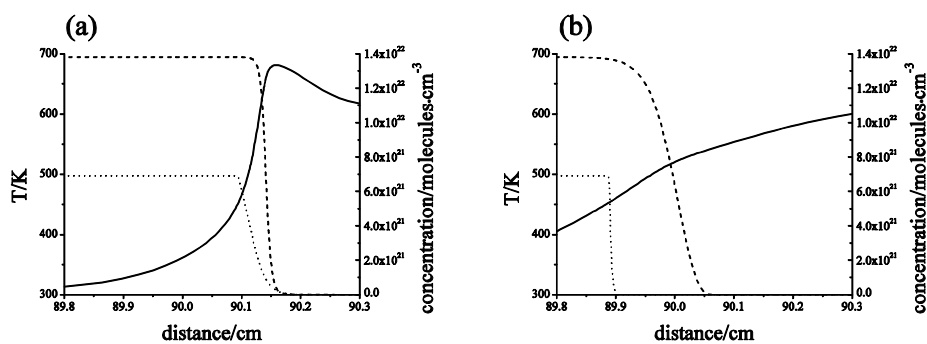


Figure 5. Spatial structure of the travelling AN combustion front for Case 3(b) of figure 3. (a) at a peak of the temperature oscillation. (b) at a minimum of the temperature oscillation. Solid line – Temperature, dashed line – AN, dotted line – water x 5.

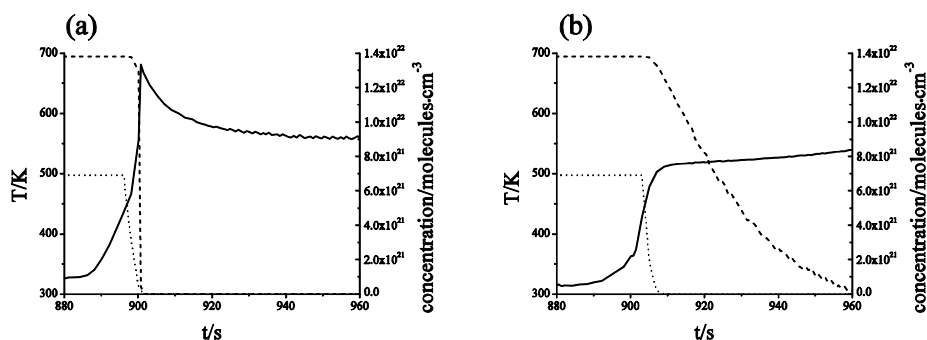


Figure 6. Temporal structure of the travelling AN combustion front for Case 3(b) of figure 3 at a fixed point in space. (a) at the peak of a temperature oscillation (90.16 cm). (b) at a minimum of the temperature oscillation (90.0 cm). Solid line – Temperature, dashed line – AN, dotted line – water x 5.

At the point at which the temperature of the frontal zone is at its maximum (Figures 5a, 6a) the water has not totally evaporated before the AN has decomposed. The net exothermic decomposition of AN has thus been able to raise the temperature with minimum hindrance from water evaporation to a value near that at which the thermal effects of the exothermic and

endothermic decomposition processes balance each other, and the temperature gradient ahead of the front is at a maximum. The consequent strong heat diffusion leads to the situation (Figures 5b, 6b) in which the frontal temperature has reached a minimum value, and the AN decomposition front has fallen behind the evaporation front. This means that there is no water left to inhibit the AN decomposition and the temperature is able to rise again to a new peak – and so the cycle repeats.

Observed from a point fixed in space (as is more likely to be experimentally possible) the phenomenology takes the following form (Figure 6a, 6b)

1. Diffusion of heat from the imposed source (hot wall or fuel-HNO₃ reaction) causes a rise in temperature which stimulates the net exothermic AN decomposition.
2. At some temperature the saturation vapour pressure for water evaporation, P_{sat} , reaches the ambient pressure, P_{amb} , and significant evaporation begins, its endothermic effect partly offsetting the heat input from AN decomposition to an extent related to the total amount of water present and to the rate at which evaporation can occur. This latter rate is difficult to estimate, and will depend critically on the ease of bubble formation in the mixture. Importantly, it will also, by its influence on the temperature, affect the proportions of AN going down the two channels of reaction, 1 and 2, and therefore the *net* exothermicity of the AN decomposition. The temperature continues to rise, until eventually, when the AN decomposition and water evaporation are complete, it reaches a “plateau” level, T_b , consistent with the total net heat input.
3. This temperature then constitutes the “upstream” condition for the preheat zone of the following AN decomposition front. Whether this front propagates is a delicate balance of the kinetics, and any heat losses. In practice, even a small external heat loss could prevent its initiation if the T_b is too low.

Just as expected from the zero-dimensional case, the behaviour depends critically on the water fraction and the relationship of its temperature-dependent saturation vapour pressure to the ambient pressure. Using the values of the chemical kinetics and physical properties adopted earlier for the case of the decomposition of AN in solution with water, we summarise in Figure 7 the results of a large number of computations, showing the approximate location of the boundaries between the various observed phenomena. Each point represents the outcome of a computation based on equations (1-3) for the values for water content and pressure illustrated

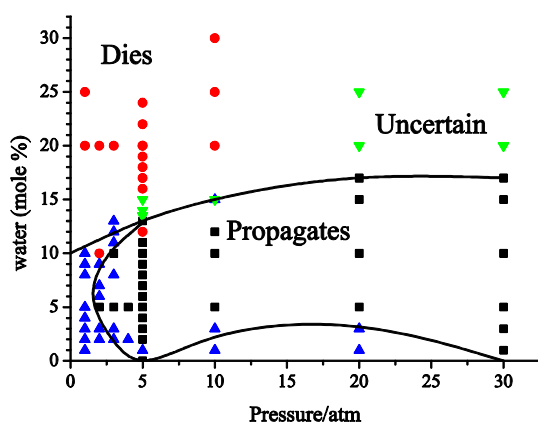


Figure 7. Regions of common AN combustion wave behaviour as a function of ambient pressure and water content. black squares – propagates, blue triangles – propagates then dies, green triangles – long time behaviour still uncertain within time range of computation, red circles – dies.

Initiation and subsequent self-propagation (or failure) of a travelling front is seen to depend critically on both total water content and ambient pressure. The outcome, propagation or non-propagation and general phenomenology of the dissociation front, is also highly sensitive to parameter values representing the competitive chemical kinetics and the physics of evaporation and heat diffusion. Since these are unlikely to be well known in any particular case, *detailed* prediction may always be difficult, even though the pattern of qualitative behaviour is robust.

The extent of the competition between the exothermic and endothermic components of the overall chemical reaction may be characterised by the “crossover temperature”, T_c , at which the thermal effects exactly cancel. This clearly establishes an upper bound on the temperature attainable without external heat input; for the chemical kinetics represented in Figures 3 and 4, this temperature is 724 K. In general the actual burnt temperature, T_b , is somewhat below this bound, influenced by the thermal capacity of the emulsion to be heated. A second reference value of interest which can establish an upper bound is the “pseudo-adiabatic” temperature, T_a , which would be attained if all the AN were to be consumed by the exothermic channel with no water; again, for this case $T_a = 661$ K. In practice the lower of T_a and T_c will constitute the bound.

To investigate the effect of varying T_c , the Arrhenius parameters of the exothermic reaction were held constant while the activation energy, E_1 , of the endothermic channel was changed. As E_1 is reduced, so is T_c and the endothermic process becomes significant at lower temperatures and consumes a larger fraction of the reactant. The impact of this on both the oscillatory nature of the propagation, the propagation speed, and the plateau temperature reached after passing of the combustion wave is illustrated in Figure 8; where for figure clarity propagating combustion waves at different times after initiation are shown.

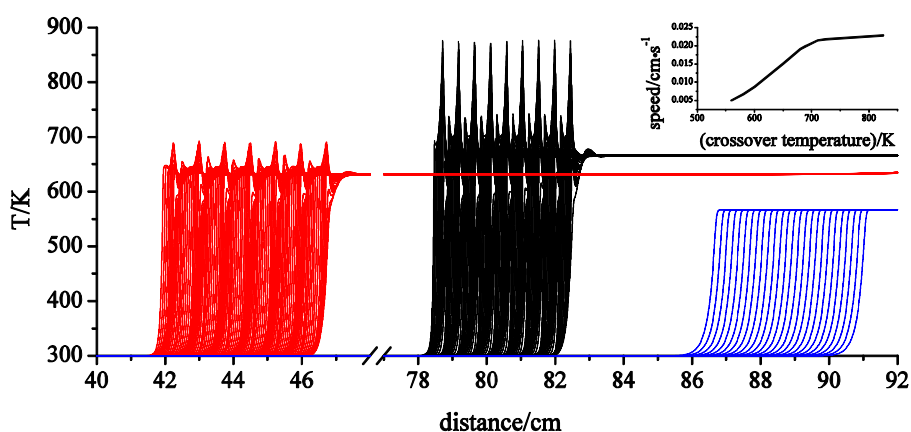


Figure 8. Propagating AN combustion waves at varying crossover temperatures created by changing the value of E_1 (for endothermic AN decomposition). Black lines – no endothermic reaction, red lines – $T_c = 724$ K, blue lines – $T_c = 600$ K.

The mean speed of propagation increases monotonically with T_c , and oscillations are very prominent at the larger values. At lower T_c values these oscillations are damped and ultimately eliminated completely for $T_c < 650$ K, and the greater fraction of AN consumed via the endothermic channel leads to a lower plateau temperature; a feature of great importance when AN decomposition is a preliminary, oxidant generating, first step in the behaviour of emulsion explosives. Ultimately, for $T_c < \sim 540$ K, the final temperature attained is too low to support

self-propagation, and the front dies. In Figure 9 we plot front speeds against the depression of the burnt plateau temperature T_b below T_c for several values of T_c , water fractions of 0, 5, 10 and 15 %, and ambient pressures of 5, 10 and 20 atmospheres.

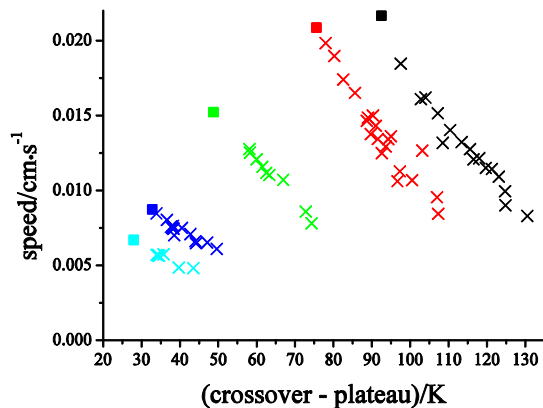


Figure 9. Predicted AN combustion wave propagation speed as a function of crossover temperature (T_c) minus burnt plateau temperature (T_b). Solid symbols – no water, open crosses – with varying water fractions up to 15 % and varying ambient pressures up to 20 atm. Black – $T_c = 724$ K, red – $T_c = 700$ K, green – $T_c = 650$ K, blue – $T_c = 600$ K, cyan – $T_c = 580$ K.

The solid square symbols denote the limiting cases with no water present and the crosses those simulations with the varying quantities of water at the specific ambient pressures. Since progress of the front is oscillatory, sometimes chaotically so, the speeds are averaged and inevitably approximate, but general trends are clear. This demonstrates an interesting characteristic in that for a range of pressures and water contents, the plots of speed suggest a unique curve for each value of the crossover temperature.

4. Theoretical Considerations

Mathematical analysis of the “ignition” phenomenon, which has been variously defined in the literature, but is taken here to be the establishment of a self-propagating exothermic dissociation process, has proved to be difficult in even the simplest contexts, particularly so when it takes place at a time and place *a priori* unknown. We adopt a simpler alternative approach, widely used in combustion problems by *assuming* a travelling front solution of constant form, and establish conditions for its existence and stability. If, as in the numerical computations earlier, we again neglect diffusion of AN and water (retaining heat diffusion), equations (1-3) simplify to

$$\frac{\partial A}{\partial t} = -(k_1 + k_2)A \quad (\text{AN decomposition}) \quad (1a)$$

$$\frac{\partial W}{\partial t} = -k_3W \quad (\text{water evaporation}) \quad (2a)$$

$$\frac{\partial T}{\partial t} = -\frac{\{(Q_1k_1 + Q_2k_2)A + Q_3k_3W\}}{C_v\rho} + D_T\nabla^2T \quad (\text{energy}) \quad (3a)$$

where A and W are the fractional concentrations of AN and water respectively. The AN decomposition, equation (1a), is modelled by simultaneous *competitive* exothermic and endothermic processes, each feeding on the AN component of the emulsion, whilst the water evaporation, equation (2a), is represented by a *parallel* endothermic process, feeding on the

water component, shown schematically in Figure1. Given that the activation energies differ; in our case $E_2 < E_1$. Influenced by the thermal capacity the available AN is thus depleted simultaneously by the two chemical reactions and the share between exothermic (X) and endothermic ($1 - X$) is controlled by temperature through the exponential dependences. The water evaporation kinetics, represented by the function $k_3(T)$, is, in contrast, extremely pressure sensitive, as we have stressed in Section 2.

Since our main concern is with the existence of travelling wave-like solutions to equations (1a,2a,3a) above, it is convenient to transform to a co-ordinate system travelling with (constant) speed c . Then if we introduce a new independent co-ordinate, $\xi = x - ct$, and at the same time introduce the ‘‘Frank-Kamenetski’’ variable

$$u = (T_a - T)E_2/RT_a^2$$

where T_a is a ‘‘pseudo-adiabatic’’ burnt temperature as defined earlier, then

$$\exp(-E_1/RT) = \exp(-v/\varepsilon)R_{21} ; \exp(-E_2/RT) = \exp(-1/\varepsilon)R_{22} ;$$

and we obtain the equations

$$cA' - (\beta_2 R_{22} + \beta_1 R_{21})A = 0 \quad (6)$$

$$cw' - R_1 w = 0 \quad (7)$$

$$D_T u'' + cu' + (\alpha_2 R_{22} + \alpha_1 R_{21})A + LR_1 w = 0 \quad (8)$$

where A' and w' represents derivatives with respect to ξ , and where

$$R_{22} = \exp(-u/(1-\varepsilon u)) \quad R_{21} = \exp(-vu/(1-\varepsilon u)) \quad R_1(u, P) \equiv k_3(T, P)$$

$$\varepsilon = RT_a/E_2 ; v = E_1/E_2 ; \alpha_1 = \exp(-v/\varepsilon)K_1 q_1 / \varepsilon T_a ; \alpha_2 = \exp(-1/\varepsilon)K_2 q_2 / \varepsilon T_a ;$$

$$q_i = \frac{Q_i}{\rho C_v} \quad i = 1, 2 ; \beta_1 = \exp(-v/\varepsilon)K_1 ; \beta_2 = \exp(-1/\varepsilon)K_2 ; w \equiv \frac{W}{\varepsilon T_a}$$

Finally, $R_1 (= k_3)$ represents the unit rate of water evaporation, and $L(u)$, ($= Q_3/\rho C_v$), is an appropriately scaled measure of the latent heat of evaporation. R_1 will of course depend sensitively on the detailed surface physics of the process, availability of bubble formation nuclei, etc, as well as on the vapour pressure, and thereby the temperature.

R_{22} (or alternatively R_{21}) may now be eliminated from equations (6-8) to obtain

$$\beta_2 (D_T u'' + cu') + \alpha_2 cA' + L\beta_2 R_1 w - (\alpha_2 \beta_1 - \alpha_1 \beta_2)R_{21} A = 0 \quad (9)$$

which, assuming that $A=A_0$, $u=u_0$, $u' \rightarrow 0$ as $x \rightarrow -\infty$, ($\xi \rightarrow -\infty$), integrates to

$$\begin{aligned} & \beta_2 (D_T u' + cu) + \alpha_2 cA + \int_{-\infty}^{\xi} L\beta_2 R_1 w d\xi^* - (\alpha_2 \beta_1 - \alpha_1 \beta_2) \int_{-\infty}^{\xi} R_{21} A d\xi^* \\ & = c(\beta_2 u_0 + \alpha_2 A_0) \end{aligned} \quad (10)$$

Then, if $A=A_b$, $u=u_b$, $u' \rightarrow 0$ as $x \rightarrow +\infty$, ($\xi \rightarrow +\infty$), we have

$$\beta_2(u_b - u_0) + \alpha_2(A_b - A_0) + c^{-1} \int_{-\infty}^{+\infty} L\beta_2 R_1 w d\xi^* = c^{-1} (\alpha_2\beta_1 - \alpha_1\beta_2) \int_{-\infty}^{+\infty} R_{21} A d\xi^* \quad (11)$$

For the Arrhenius chemistry assumed here, A_b will of course be zero, so that

$$\beta_2(u_b - u_0) = -c^{-1} \int_{-\infty}^{+\infty} L\beta_2 R_1 w d\xi^* + \alpha_2 A_0 + I, \quad (12)$$

where
$$I = c^{-1} (\alpha_2\beta_1 - \alpha_1\beta_2) \int_{-\infty}^{+\infty} R_{21} A d\xi^* \quad (13)$$

and, recalling the expression for u , we obtain the result

$$T_b = T_0 - A_0 q_2 + c^{-1} \int_{-\infty}^{+\infty} L R_1 W d\xi^* - J \quad (14)$$

for the burnt (plateau) temperature T_b ,

where
$$J = c^{-1} K_1 \exp(-v/\varepsilon) (q_2 - q_1) \int_{-\infty}^{+\infty} R_{21} A d\xi^* . \quad (15)$$

Note that because the wave is going from right to left in this work, the speed of the front c is negative so that with q_2 negative and c negative, J is in fact positive and all the terms in (14) other than the first term represent a reduction in burnt temperature (as one would expect). But the actual amount of reduction in temperature is not *a priori* known. The presence of the integral expressions in (14) reflects the dependence of T_b on the whole time history and spatial distribution of the reaction and evaporation processes. In this case of *competitive* dissociation processes it is not possible to express T_b solely in terms of the total consumption of A and W , as would be possible for independent *parallel* reactions, which would yield the second and third terms on the right hand side of equation (14). In our case the effect arising from the fraction of AN consumed by the competing endothermic reaction, is also present. Its magnitude, however, depends on the value of the integral, which links in a convoluted way the temperature and AN fields and is sensitively dependent through v and ε on the chemical kinetics.

Other sensitivities are captured in the factors of the constant multiple of the integral, which represent the wave speed, the pre-exponential factor of the endothermic reaction, and the total endothermic effect of the “theft” of AN by the endothermic reaction (not only by the direct cooling effect (q_1), but also the loss of AN which would otherwise have reacted exothermically (q_2)).

Even in the absence of water ($W = 0$) the integral is present; additionally however, for the emulsion, the water component is, through the effect of its (endothermic) evaporation on the temperature field and hence on I , able to exert an effect on the division of AN between the exothermic and endothermic channels of decomposition. Specifically, if we denote by X and $1 - X$ the fractional rates at which A is consumed by the exothermic and endothermic reactions respectively, it is readily seen that we must have, at a temperature T ,

$$X = 1/(1 + v), \quad 1 - X = v/(1 + v), \quad (16)$$

where

$$v = (K_1/K_2) \exp\{-(E_1 - E_2)/RT\} \quad (17)$$

Moreover, since significant water evaporation occurs only when P_{sat} (associated with a temperature T_{sat}) is near to or above the ambient pressure, P_{amb} , and since P_{sat} itself is strongly temperature dependent, the endothermic effect of water evaporation is significant in the overall process only when the temperature of the mixture, T , reaches or exceeds $T_{\text{sat}}(P_{\text{amb}})$. Thus, if P_{amb} is low, the water evaporates at a relatively low temperature, effectively holding the temperature depressed at a level at which the exothermic channel of AN dissociation dominates; if it evaporates at a higher temperature (ie higher P_{amb}) the endothermic channel takes a larger share of the more rapid AN dissociation, thus decreasing the net exothermicity of the total dissociation chemistry. However the overall process is further complicated by the decrease of latent heat with increasing temperature, and for the chemical kinetics used in our numerical examples this decrease in endothermicity is greater than the decrease in chemical exothermicity. This is the likely reason for the higher burnt temperature, T_b , and therefore greater possibility of a self-propagating front at higher pressures, as widely observed in the explosives industry through the concept of a minimum burning pressure (MBP).

This complex picture may be illustrated more precisely if we make the extreme assumption that the rate of water evaporation is so great that it can all evaporate at T_{sat} , its endothermic effect exactly balancing the net exothermic effect of AN decomposition at that temperature. This behaviour is illustrated schematically in Figure 10.

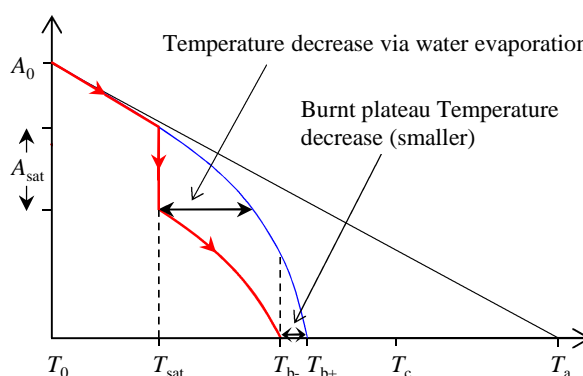


Figure 10. Schematic representation of temperature change as AN consumed illustrating the effect on T_b of competitive reactions alone (blue line) and with water evaporation in addition (red line) for the case $T_c < T_a$.

Thus, if we denote by A_{sat} the total amount of AN consumed at T_{sat} , we must have

$$A_{\text{sat}}[X_{\text{sat}}Q_2 + (1 - X_{\text{sat}})Q_1] = L(T_{\text{sat}})W_0 \quad (18)$$

where X_{sat} is the fraction of A going down the exothermic channel at T_{sat} , whilst for the regions at lower (L) and higher (H) temperatures, we must have

$$A_L[X_LQ_2 + (1 - X_L)Q_1] = \rho C_v(T_{\text{sat}} - T_0)$$

and

$$A_H[X_HQ_2 + (1 - X_H)Q_1] = \rho C_v(T_b - T_{\text{sat}}) \quad (19)$$

respectively, where $X_{H,L}$ are the total integrated fractions of A going down the exothermic channel in the regions $T_0 < T < T_{\text{sat}}$ and $T_{\text{sat}} < T < T_b$. These are of course *a priori* unknown, but note that throughout the lower region we have $X > X_{\text{sat}}$, and in the upper region $X < X_{\text{sat}}$. Clearly

the net heat production of the whole process, as measured by $T_b - T_0$, is maximised when the sum of the quantities

$$A_L[X_L Q_2 + (1 - X_L)Q_1] + A_H[X_H Q_2 + (1 - X_H)Q_1]$$

is maximised, subject to the condition

$$A_{\text{sat}} + A_L + A_H = A_0 \quad (20)$$

We have at (18) above an explicit expression for A_{sat} , in which everything is known in terms of T_{sat} . If we further assume that the initial fractions A_0 of AN and W_0 of water in the mixture are y and $1 - y$ respectively, this expression becomes

$$A_{\text{sat}} = L(T_{\text{sat}})[(1 + \nu)/(Q_2 + \nu Q_1)] [(1 - y)/y] \quad (21)$$

which neatly encapsulates the effects of pressure on the chemistry, through $T_{\text{sat}}(P_{\text{sat}})$ and hence ν_{sat} , the water content, through y , and the varying endothermic effect of its evaporation through the latent heat $L(T_{\text{sat}})$. Note that the latent heat, $L(T_{\text{sat}})$, decreases with temperature, whilst the chemical kinetics term in the first square bracket, increases; increasing water (decreasing y) of course always increases the expression for A_{sat} . For temperatures well below T_c the decrease in L dominates the increase in the chemical kinetics term, so A_{sat} decreases with increasing T_{sat}

The expressions for A_L and A_H are implicit, still dependent on the whole spatiotemporal distribution through the integrated quantities X_L and X_H , and subject to the constraint (20) above, but responsible for the value of the burnt temperature T_b , since

$$A_L[X_L Q_2 + (1 - X_L)Q_1] + A_H[X_H Q_2 + (1 - X_H)Q_1] = \rho C_v (T_b - T_0)$$

which, using (20), may be written as

$$\rho C_v (T_b - T_0) = (Q_2 - Q_1)(A_L X_L + A_H X_H) + Q_1(A_0 - A_{\text{sat}}) \quad (22)$$

equivalent, when the integrals are appropriately expressed for this special case, to the more general form in equation (15) above.

Overall it is clear that if $1 - x$ is everywhere very small, the fraction of A going down the exothermic channel, and therefore the value of T_b , are both maximised for higher values of T_{sat} , as occur for higher pressures. Note that this is not necessarily the case as T_{sat} approaches T_c , as may occur at very high pressures, when the value of $1 - x$ may not be small everywhere.

In the more realistic case, where the water evaporation takes place over a range of $T > T_{\text{sat}}$, we should expect similar arguments to hold, perhaps even more strongly since the fraction of A “wasted” on the endothermic channel at these higher temperatures is greater than at T_{sat} . Making the reasonable assumption that higher T_b leads to more likely self – supporting propagation of a reaction front, these results are entirely consistent with the numerical results demonstrated in Figure 3. In particular the widely observed phenomenon of a minimum burning pressure is exhibited, though it seems likely that in practical situations the presence of multiple additives may complicate the interpretation of cause and effect.

Finally, if all the water is able to evaporate before the AN is totally consumed, the temperature gradient through the front will be monotonic, equilibrating at a value below T_c when all the AN is consumed. If, on the other hand, water is left over after the AN is totally consumed, the final temperature will be reduced by the subsequent unbalanced evaporation of the water. In either case, the speed of propagation of the front will be influenced by the forward diffusion of heat

into the preheat zone, and this depends sensitively on the full spatiotemporal evolution of the temperature field.

5. Summary and Discussion

We have explored, through a series of numerical experiments, the phenomenology of ignition and subsequent burning characteristics of condensed phase materials in which the simplest lumped chemical kinetics model comprises two reactions, one exothermic and one endothermic, each competing for the same reactive source material. Such competitive reactions differ from the case of parallel reactions, in which concurrent exothermic and endothermic processes feed on separate constituents of the source material, in that the two reactions are coupled materially as well as thermally. Since our initial motivation was the initial burning and subsequent explosion of emulsion, AN based, explosives, most of our numerical simulations have included, in addition to the competitive model for the AN decomposition, an extra endothermic process associated with evaporation of the water component of the emulsion. Our principal numerical results are

1. Strong pressure dependence, both of the initial ignition and of the subsequent combustion phenomenology
2. Extreme sensitivity, especially in the occurrence/non-occurrence of ignition, to the chemical kinetics, which are in most practical situations poorly defined
3. Regimes of qualitative behaviour consistently reproduced, and broadly consistent with other extensive work on cooled flames, etc., but with some distinctive, and even counterintuitive features
4. Common occurrence of oscillatory propagation, varying from regular periodicity to “chaotic”.

In addition, a very preliminary study of an ODE model for a travelling combustion front demonstrates more explicitly

- 5 The roles of the various physical and chemical properties and processes
- 6 The importance of the ambient pressure, through its effect on the evaporation of the water content, in mediating the division of AN decomposition down the competing channels
- 7 The complex dependence of observable features, for example burnt temperature, on the whole detailed spatiotemporal history of the reaction

One unexpected and counterintuitive feature of the numerical results was the possibility that the addition of a totally endothermic process, the evaporation of the water content of the emulsion, might lead to an increase net exothermicity of the AN decomposition, and, perhaps, even the overall exothermicity of the process, as indicated by the final burnt temperature. As we have seen from equation (12), the total effect of adding water includes the subtle influence it can have on the division of the AN decomposition down the competing exothermic and endothermic channels. This can actually reduce the value of the integral I through the detailed distribution of temperature and AN fraction throughout the whole travelling front, so that, for small water fractions, the decrease in the endothermic final term of equation (12) can outweigh the increase in net endothermicity of the first two terms. In effect there is a trade-off between the endothermicity of the increased water fraction and the combined exothermicity and direct consumption of AN which is thereby avoided; it may be more effective to use the exothermic channel for AN to counteract the effects of water evaporation, especially for relatively high values of T_{sat} , than to counteract the dual effects of the endothermic channel. This ceases to be

true when the initial water component becomes larger, as the concomitant smaller value of A_0 , and consequently A , lessens the potential effect of the integral term; detailed evaluation of these effects for a variety of models for water evaporation will form the subject of a subsequent paper, but the general character of the process could have useful applications in, for example, optimising the output of a specific product of the total reaction.

More generally, the results show extensive regions of parameter space in which the propagation of the front is oscillatory. In a broad sense, the behaviour changes from failure to ignite to almost steady propagation, then through a region of regular oscillations to a region of large, irregular oscillations which sometimes culminate in extinction, as the value of $T_c - T_b$ increases; a specific example is shown in Figure 7. Though the dominance of oscillatory behaviour fits well with other results for large Lewis number situations [16], better understanding of the detailed mechanisms and controlling influences awaits further investigation.

Acknowledgment

We thank Dr S.K. Chan for introducing us to this very interesting chemical problem and for initial financial support from Orica.

References.

1. Jones, D.E.G., Feng, H., Mintz, K.J. and Augsten, R.A. 1999 Parameters Affecting the Thermal Behaviour of Emulsion Explosives. *Thermochimica Acta* **33**, 37-44.
2. Goldthorp, S., Turcotte, R., Badeen, C.M. and Chan, S.K. 2008 Minimum Pressure for sustained Combustion in AN-based Emulsions. *Proceedings of the International Pyrotechnics Seminar*, **35**, 385-394.
3. Turcotte, R., Goldthorp, S., Badeen, C.M., Johnson, C., Feng, H. and Chan, S.K. 2009 Influence of Physical Characteristics and Ingredients on the Minimum Burning Pressure of Ammonium Nitrate Emulsions. *Proceedings of the International Pyrotechnics Seminar*, **36**, 197-206.
4. Brill, T.B., Brush, P.J. and Patil, D.G. 1993 Thermal Decomposition of Energetic Materials. 58. Chemistry of Ammonium Nitrate and Ammonium Dinitramide Near the Burning Surface Temperature. *Combustion and Flame*, **92**, 178-186.
5. Sinditskii, V.P., Egorhev, V.Y., Levshenkov, A.L. and Serushkin, V. 2005 Ammonium Nitrate Combustion Mechanism and the Role of Additives. *Propellants, Explosives, Pyrotechnics* **30**, 269-280.
6. Sun, J., Sun, Z., Wang, Q., Ding, H., Wang, T. and Jiang, C. 2005 Catalytic Effects of Inorganic Acids on the Decomposition of Ammonium Nitrate. *J. Hazardous Materials* **B127**, 204-210.
7. Gunawan, R. and Zhang, D. 2009 Thermal Stability and Kinetics of Decomposition of Ammonium Nitrate in the Presence of Pyrite. *J. Hazardous Materials* **165**, 751-758.
8. Simoes, P.N., Pedroso, L.M., Portugal, A.A. and Campos, J.L. 1998 Study of the Decomposition of Phase-stabilized Ammonium Nitrate by Simultaneous Thermal Analysis. *Thermochimica Acta* **319**, 55-65.

9. Olszak-Humienik, M. 2001 On the Thermal Stability of some Ammonium Salts. *Thermochimica Acta* **378**, 107-112.
10. Ball, R., McIntosh, A.C. and Brindley, J. 1999 Thermokinetic Models for Simultaneous Reactions; A Comparative Study. *Combust. Theory and Modelling* **3**, 447-468.
11. Gray, B.F., Kalliadasis, S., Lazarovici, A., Macaskill, C., Merkin, J.H. and Scott, S.K. 2002 The Suppression of an Exothermic Branched-chain Flame through Endothermic Reaction and Radical Scavenging. *Proc. R. Soc. A* **458**, 2119-213.
12. Simon, P.L., Kalliadasis, S., Merkin, J.H. and Scott, S.K. (2004) Stability of Flames in an Exothermic-endothermic system *IMA J. App. Maths* **69**, 175-203.
13. Hmaid, A., McIntosh, A.C. and Brindley, J. 2010 A Mathematical Model of Hotspot Condensed Phase Ignition in the Presence of a Competitive Endothermic Reaction. *Combust. Theory and Modelling* **14**, 893-920.
14. Sharples, J.J., Sidhu, H.S., McIntosh, A.C., Brindley, J. and Gubernov, V.V. 2012 Analysis of Combustion Waves Arising in the Presence of a Competitive Endothermic Reaction. *IMA J. App. Maths* **77**, 18-31.
15. Gubernov, V.V., Sharples, J.J., Sidhu, H.S., McIntosh, A.C. and Brindley, J. 2012 Properties of combustion waves in the model with competitive exo-and endothermic reactions. *Journal of Mathematical Chemistry* **50**, 2130-40.
16. Mercer, G.N., Weber, R.O. and Sidhu, H.S. 1998 An Oscillatory Route to Extinction for Solid Fuel Combustion Waves due to Heat Losses. *Proc. R. Soc. A* **454**, 2015-2022.
17. McIntosh, A.C., Weber, R.O. and Mercer, G.N. 2004 Non-adiabatic combustion waves for general Lewis numbers: wave speed and extinction conditions. *ANZIAM J.* **46**, 1-16.
18. Manelis, G.B., Nazin, G.M., Rubtsov, Yu. I. and Strunin, V.A. 2003 *Thermal Decomposition and Combustion of Explosives and Propellants*. pp. 175-187. Taylor and Francis
19. Wagner, W. 1973 New vapor pressure measurements for argon and nitrogen and a new method for establishing rational vapor pressure equations. *Cryogenics* **13(8)**, 470-482.
20. Pitzer, K.S. 1955 The Volumetric and Thermodynamic Properties of Fluids. I. Theoretical Basis and Virial Coefficients. *J. Am. Chem. Soc.* **77**, 3427-3433.
21. Campbell, A.N., Fishman, J.B., Rutherford, G., Schaefer, T.P. and Ross, L. 1956 Vapor Pressures of Aqueous Solutions of Silver Nitrate, of Ammonium Nitrate, and of Lithium Nitrate. *Can. J. Chem.* **34**, 151-159.
22. The NAG Fortran Library (2013), The Numerical Algorithms Group (NAG), Oxford, United Kingdom www.nag.com
23. Pennington, S.V. and Berzins, M. (1994) New NAG library software for first-order partial differential equations *ACM Trans Math Software* **20**, 63-99.
24. Weber, R.O., Mercer, G.N., Sidhu, H.S. and Gray, B.F. 1997 Combustion Waves for Gases ($Le = 1$) and Solids ($Le \rightarrow \infty$). *Proc. R. Soc. A* **453**, 1105-1118.